



Wideband optical absorber based on plasmonic metamaterial cross structure

Mohammad Reza Soheilifar¹

Received: 5 August 2018 / Accepted: 7 November 2018 / Published online: 14 November 2018
© Springer Science+Business Media, LLC, part of Springer Nature 2018

Abstract

The optical absorber with Fano response is valuable for various applications such as solar cells or optical sensors. In this paper, we have modeled an optical plasmonic metamaterial absorber which contains a broken cross as an elementary cell along with four rectangular loads to improve the absorbance and achieve a Fano response within a wide bandwidth at 190–245 THz (25%). The bandwidth of the proposed structure is more than conventional metamaterial absorbers. The prototype absorber has a remarkable enhancement in the electric field in comparison with the simple cross model and the reflection value has reduced to -47 dB. The parametric studies show how the gap capacitance controls the bandwidth, resonance frequency and the reflection value of the absorber, therefore we can consider this technique as a way to enhance the metamaterial absorber's bandwidth. The proposed structure can be used as an optical refractive index sensor while the Fano line-shape provides a higher figure of merit (FOM) compared with many others. For this structure, the FOM has obtained as 10,660. The Finite Integration Technique with Perfect Boundary Approximation used for the simulation.

Keywords Fano resonance · Plasmonic · Metamaterial · Absorber

1 Introduction

The progress in micro and nanofabrication technology has resulted in new aspects for researches in the optical spectrum (Yang et al. 2011). Therefore, the related frequency wavelength of these structures places in the range of terra-hertz (THz) and optics (Yang et al. 2011; Lu et al. 2013). This new topic is called plasmonic and oriented to the interaction of a metal and dielectric in the optical frequency when they are excited by an electromagnetic wave (Nozhat and Granpayeh 2012).

Surface plasmon polaritons (SPPs) can be excited by both electrons and photons (Mayer and Hafner 2011). They have placed at the interface of metal and dielectric (Chiadini et al. 2016). Basically, the energy of photons is absorbed by the electrons

✉ Mohammad Reza Soheilifar
rsoheilifar@ee.kntu.ac.ir

¹ Faculty of Electrical Engineering of Naval Sciences, Imam Khomyini University of Nowshahr, Nowshahr, Iran

of the metal. These coupled plasmon-photon elements are named plasmon polariton (Hedayati et al. 2014). The dipolar field has established on the edge of the outer part of the particle while it can scatter the absorbed energy from the photons. Therefore, the metal layer shows negative permittivity (Giannini et al. 2011).

Some new devices have been designed in the terahertz and optic domains based on plasmonic properties. Studies on the absorption properties of these structures have been considered for designing absorbers for terahertz spectrum with multiband properties (Zare et al. 2017). On the other hand, the Nano-antennas are typically designed based on small particles for miniaturizing and increasing the resonant frequency.

Numerous applications of optical Nano-antennas in designing various devices including optical sensors (Tittl et al. 2012), terahertz detectors (Watanabe et al. 2012) and solar cells (Muhammad et al. 2015) prove their significance.

Sensors (Cetin et al. 2015), detectors (Hu et al. 2011) and solar cells (Simovski et al. 2013) composed of Nano-antennas with active materials are subjects of concern in the field of optics, because of changing field intensity and producing more charges by active elements (Bazgir et al. 2018). Therefore, changes in the electric field or resonance frequency are known as the basic factor for designing refractive index sensors (Zarrabi et al. 2017).

Metamaterials have properties which are not found naturally available in other materials. These structures have been considered so much during the last decade because of the great variety of properties and applications (Xu et al. 2014).

Typically, metamaterials have been considered for perfect absorbers (PAs) in two main categories. In the first group, the metamaterial has been used as an element with large effective permittivity and permeability in conductors. In the second category, the PAs have been made based on metamaterial elements which are closely coupled with a ground plane. Both layers are separated by a dielectric spacer layer (Durmaz et al. 2018). Recently, various models of Nano-antennas (absorbers) have been developed for optical sensing with single or multi resonances (Durmaz et al. 2018; Adato et al. 2011, 2015). However, the narrow bandwidth has remained as a main drawback.

Metasurfaces are considered as 2D metamaterial structures with subwavelength dimensions which are used in various applications in the optical regime, for example, in the optical mirror and reflect surface (Ghasemi and Choudhury 2016) and the optical polarizer (Kang et al. 2013). Two major types of the metasurfaces are suggested as a slot and complementary formation for polarizer (Heydari et al. 2017; Zhao and Alù 2011). For designing metasurface as a polarizer, various models of nanoparticles are studied such as SRR as a metamaterial based on Babinet theory (Falcone et al. 2004). Metasurfaces based on coupling of plasmonic response and second harmonic generation with T shape element (Gomez-Diaz et al. 2015) and various shapes of metasurface are compared such as I, V and C shapes for generating circular polarization (Meinzer et al. 2014).

In addition, various simple or complicated shapes of unit cells are noticed for developing absorbers in microwave region or for antenna designing among THz to optical regime such as linear disk array for bio-sensing (Liu et al. 2010), wideband polarization independent perfect metamaterial (Rufangura and Sabah 2016), plasmonic cylindrical slots (Withayachumnankul et al. 2014) and hexagonal cylindrical structure with Fano resonance for optical sensing (Mirzabeygi and Naser-Moghadasi 2018).

In this paper, we have studied a novel broken cross absorber with wide bandwidth for optical sensing. Rectangular loads are added to this structure. We can see the enhancement of the bandwidth and decrement of the reflection value to -47 dB. This reflection proves that the structure has a proper absorption at 230 THz. Moreover, we have compared this

structure with the simple cross model to exhibit the benefits of the broken cross model in comparison with the simple cross model.

2 Absorber design and background theory

The Commercial software, CST Microwave Studio has been used to simulate the characteristics of the proposed absorber using time domain simulation with periodic boundary conditions, and also open boundary is selected as a conventional PML to a height of $\lambda/4$ for 3D simulations. Simulation produced the complex frequency dependent S-parameters, S_{11} and S_{21} , where $R(\omega) = |S_{11}|^2$, $T(\omega) = |S_{21}|^2$ and $A(\omega) = 1 - |S_{11}|^2 - |S_{21}|^2$ are the reflectance, transmittance, and absorbance respectively (Jahangiri et al. 2017). We have used wave ports for excitation of the absorber.

Figure 1 shows the proposed absorber which has three layers. The gold material is used for the top and bottom layer and the SiN dielectric is placed between them as a spacer. The Palik model utilized for the gold layer. The Palik and Johnson models are provided with experimental measurement and some researches compared with Drude model (Etchegoin et al. 2006). For the Drude model, the ϵ_m is for Au (gold) where

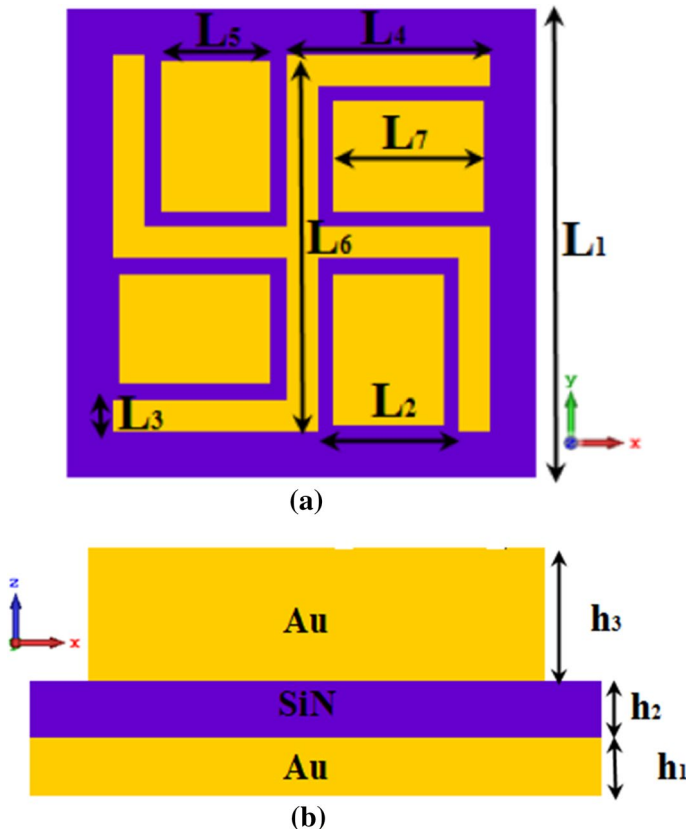


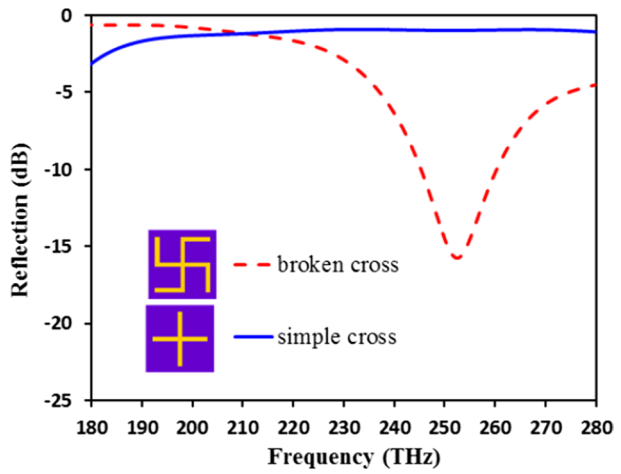
Fig. 1 The suggested structure and dimensions **a** from top view, **b** side view of the absorber (Au/SiN/Au)

$\epsilon_m = \epsilon' + i\epsilon'' = (1 - \omega_p^2/(\omega^2 + \gamma^2)) + i \gamma \omega_p^2/\omega (\omega^2 + \gamma^2)$, with $\omega_p = 9.1$ eV and $\gamma = 0.018$ eV (Farmani et al. 2018). Moreover, the refractive index of SiN is assumed 1.98.

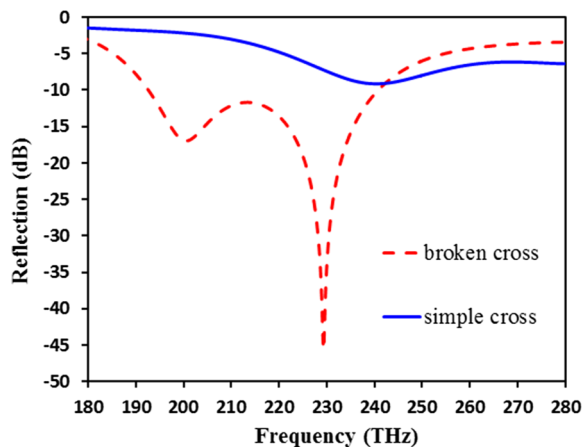
Figure 1a shows the top view of the absorber and as presented here the structure contains two sections. The main section is a broken cross structure with four rectangular loads locating inside of the cross shape. The widths of the final model are $L_1 = 300$ nm, $L_2 = 90$ nm, $L_3 = 20$ nm, $L_4 = 130$ nm, $L_5 = 60$ nm, $L_6 = 240$ nm and $L_7 = 96$ nm. Figure 2 (b) shows the side view and height of the absorber at which $h_1 = 60$ nm, $h_2 = 50$ nm, and $h_3 = 60$ nm.

Furthermore, the symmetrical structure of the absorber provides independence to the incident wave polarization, and we can neglect this factor.

Fig. 2 The reflection of the structure of simple cross and broken cross **a** without rectangular loads, **b** with rectangular loads



(a)



(b)

3 Simulation result and discussions

We have studied two models of the absorber. The first structure is the simple cross while the second model is a broken cross, then we have used the load for both structures. The reflection of the prototype absorber has been presented in Fig. 2a, b. The Fig. 2a shows the reflection of the basic structure which contains the cross structure. Here, we have compared the reflection of the simple cross and the broken cross structures. It can be perceived that the simple structure has the higher reflection of -2 dB while for the broken cross structure the reflection reduced to -15 dB at 255 THz.

Actually, we should consider that small arm in the broken cross (L_4) plays important role for increasing the capacitance and inductance of the cross structure simultaneously. In other words, the simple cross has a resonance at higher frequency which is out of our study spectrum.

Moreover, when the rectangular loads have added to the structure the, reflection improved drastically. However, most of effects happen for the broken cross structure. Figure 2b shows the reflection of the simple cross and broken cross with loads. As illustrated, for the simple structure with loads, the reflection is reduced around 4 dB, but this reflection has not sufficed. On the other hand, for the broken cross with loads, we can see a great reduction to -47 dB. In addition, the frequency has reduced and the bandwidth has increased more than 100%, which covers 190–245 THz with the Fano shape and this structure can be useful for bio-sensing.

Apparently, in the final structure, we have two main capacitances between the loads and the broken cross structure the combination of which gives us a structure with dual-band characteristic and provides a wide bandwidth quality.

The electric field is investigated for both simple cross and broken cross at 200 THz. As shown in Fig. 3a, the electric field gets concentrated in the gaps between the rectangular loads and the cross structure. In this structure, the maximum electric field is about 165 dB. When the broken cross structure combines with the rectangular loads, so, the length of the cross and gaps is increased more than those in the simple cross. Therefore, the reduction of the resonant frequency is predictable. According to Fig. 3b, the electric field concentrates between the loads and cross structure. For this structure, the maximum electric field increased up to 180 dB, so the electric field enhanced about 15 dB.

Moreover, as illustrated in Fig. 3, the metal layer under the SiN substrate can restrict the electric field transmission. This layer thickness is more than the skin depth and therefore the electric field cannot penetrate in this layer.

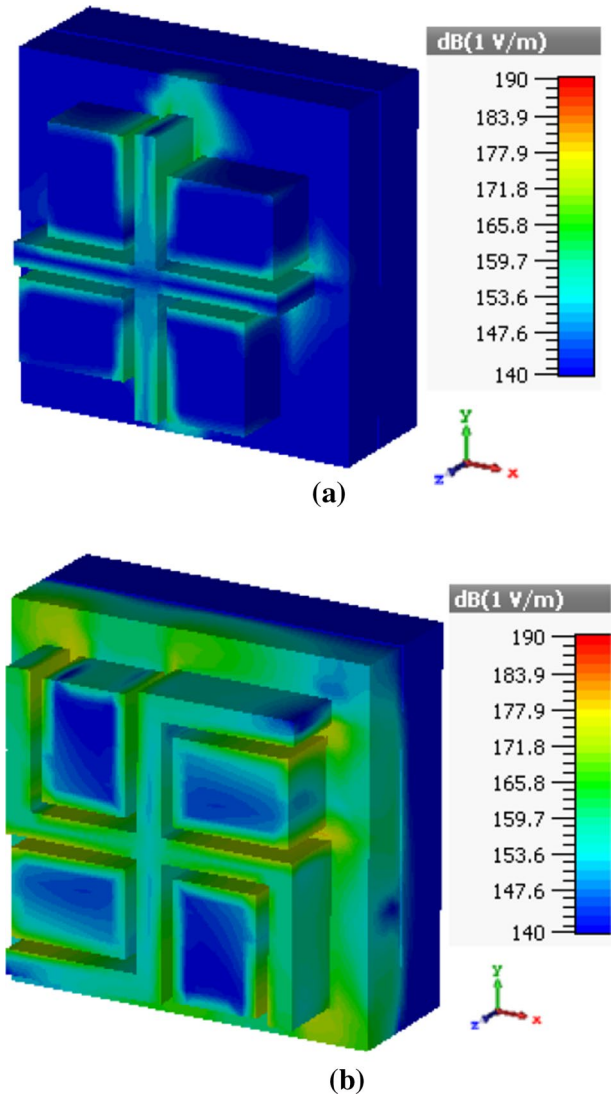
4 Parametric study of the absorber

Since the effect of the cross structure and rectangular loads are more than other factors, in this work we have selected the length of the broken cross arm (L_4), the length of the loads (L_7) and the gaps between loads and cross structure for parametric study.

4.1 The cross length effect

As mentioned, the lengths of the broken arms have impacts on the saved energy in the absorber. We have checked the effect of the arm's length (L_4) on the reflection of the

Fig. 3 The electric field enhancement for both structures at 200 THz **a** for simple cross, **b** broken cross



absorber and as shown here, by reducing L_4 from 130 to 90 nm, the reflection decreased to -6 dB and bandwidth reduced drastically. Figure 4 shows the comparison of the reflection of the final model for 90, 110 and 130 nm as the length of the L_4 .

4.2 The loads length effect

The rectangular loads length also is important for controlling the energy in the gaps. By reducing the length of the rectangular box, the gaps and the capacitance between the box and cross element decreased. Therefore, the resonance will shift to the higher frequencies according Fig. 5. As presented here, by decreasing the length from 96 to 80 nm, the second resonance has shifted from 230 to 250 THz and the bandwidth of the absorber is increased.

Fig. 4 The reflection of the absorber for various lengths of the broken arm (L_4)

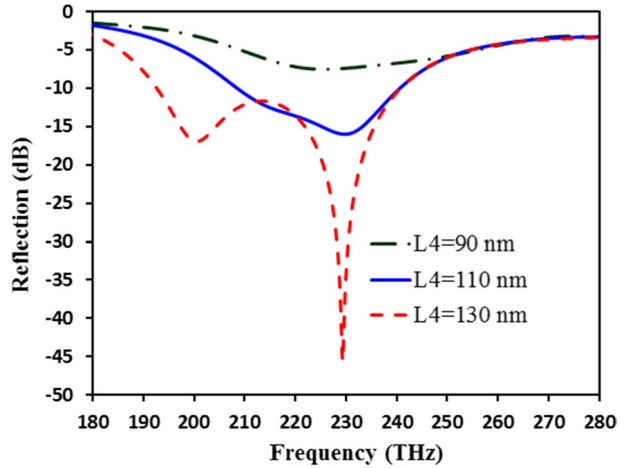
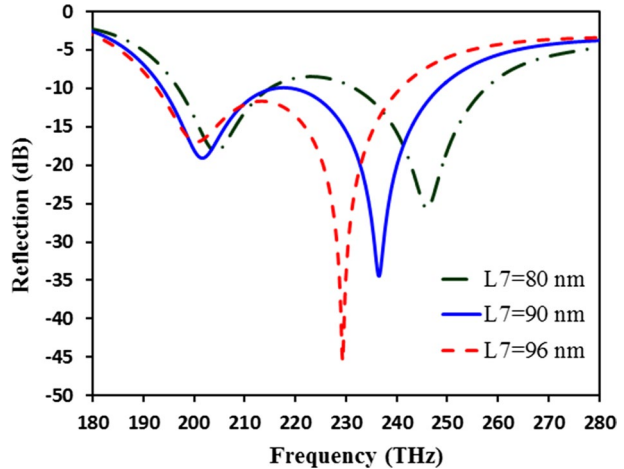


Fig. 5 The reflection of the absorber for various lengths of the rectangular loads (L_7)

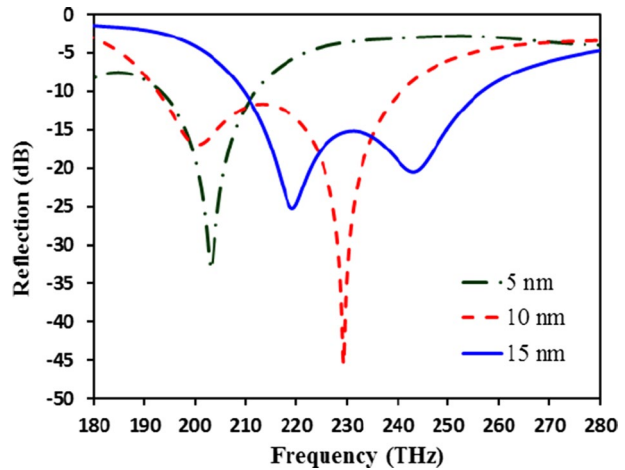


However, the reflections in some part of the spectrum have increased to -8 dB for 80 nm. So, we can control the resonance and bandwidth of the absorber by these gaps.

4.3 The gaps effect

In addition, we can control the capacitance by the width of the gaps and the comparison between various gaps presented in Fig. 6. As shown here, increase of the gaps leads to a reduction in the capacitance. In this case the resonance is shifted to a higher frequency and simultaneously the maximum value of the reflection reduced while as it can be observed, for 5 nm the increasing reflection is -8 dB, for 10 nm is -11 dB and for 15 nm it is -15 dB. Therefore, we can control the bandwidth of the absorber by variation of the gaps in addition to the length of the loads (L_7).

Fig. 6 The reflection of the absorber for various lengths of the gap between the arms and rectangular loads



5 Comparison with other research

The optical absorbers have been designed for various applications such as optical imaging, bio-sensing (Liu et al. 2010) and optical cloak (Nouri-Novin et al. 2018). We have compared the prototype model with some previous structures and we have investigated the bandwidth, frequency and the minimum value of the reflection. As shown in Table 1 most of the models exhibit a limited bandwidth between 3 and 10%. However, our proposed structure has a higher bandwidth at the optical domain and can be modified for the solar cell by changing the dimension of gaps as shown in Figs. 5 and 6.

In addition, some other structures such as Nano cylindrical cavity model (Withayachumnankul et al. 2014) have been suggested for wider bandwidths around 30%. However, this structure has been modified for THz application and it is not appropriate for optical spectrum.

Moreover, the other type of absorber like the graphene unit cells have been investigated for wide bandwidth at THz range while the bandwidth has doubled (Barzegar-Parizi 2018), but in the optical range graphene material is not suitable and typically they show lower absorption and bandwidth (Cen et al. 2018; Chen et al. 2018).

Table 1 The comparison of the prototype absorber with previous researches

	Minimum reflection (dB)	Bandwidth (%)	Frequency (THz)
This work	-47	25	190–245
Ref. Liu et al. (2010)	-45	5	180
Ref. Rufangura and Sabah (2016)	-45	7	560–600
Ref. Withayachumnankul et al. (2014)	-58	30	1.16
Ref. Mirzabeygi and Naser-Moghadasi (2018)	-17	3	148–152
Ref. Jahangiri et al. (2017)	-25	6	150–160
Ref. Nouri-Novin et al. (2018)	-16	11	142–160

The comparison of the reflection of the proposed structure with the other models is presented in Table 1 and results show that this structure can expeditiously work as an ideal absorber with a reflection value of more than -47 dB for the final model.

6 Refractive index sensing application

The optical absorbers (Jahangiri et al. 2017) and nano-antennas (Heydari et al. 2017) can be utilized for optical sensing and the spectroscopy systems, while the biological material covers the absorber and the frequency and the value of reflection will change. We can consider these changes as a factor for material detection similar to microwave sensors (Jafari and Ahmadi-Shokouh 2018). The figure of merit can be obtained based on the variation of the reflection value, frequency shift and bandwidth (Zheng et al. 2017). We can see here the frequency shift, which is mostly due to capacitive changes in the absorber. In fact, the change in permittivity leads to a change in capacitive properties.

In this section, we have covered the absorber surface with materials which have refractive indices values of 1–1.2 with the thickness of 100 nm. Figure 7 shows the absorber in touch with the material layer for sensing the refractive index.

Figure 8 shows the reflection for various material loads with refractive indices in the range of 1–1.2. As shown here, the material variation has nonlinear effect on the reflection value and reduced the frequency and bandwidth of the reflection. Here, the FOM is calculated by (1) while the “ I ” is the reflection intensity, “ ΔI ” is the intensity change and the “ Δn ” is the index change.

$$FOM_I = \text{Max} \left[\frac{\Delta I}{I \Delta n} \right] \quad (1)$$

Fig. 7 The absorber with material layer which coat the metal layer for refractive index sensing

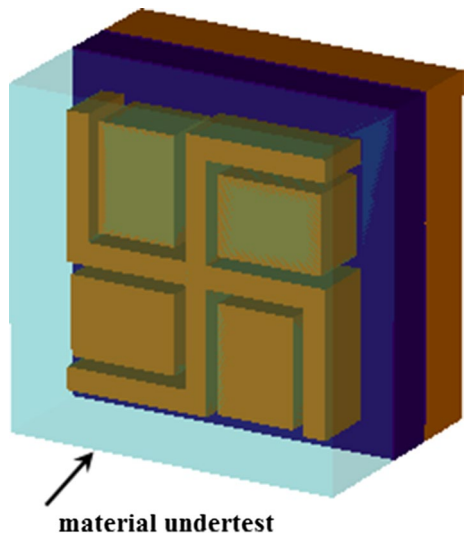
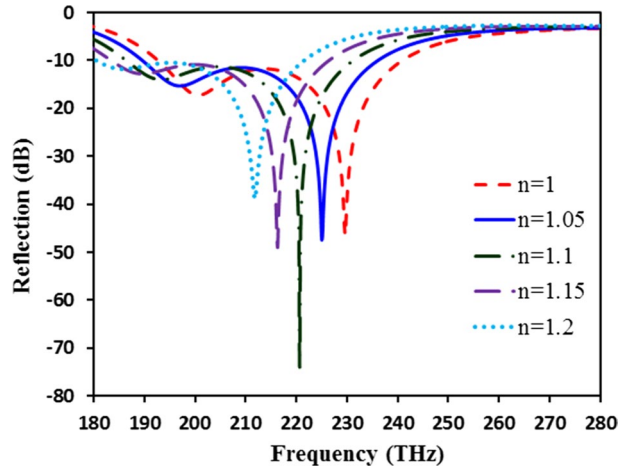


Fig. 8 The reflection for various material loads in the range of $n = 1-1.2$



As an example, at $n=1.1$ we have the minimum reflection value which is around 0.000198 (I) and the ΔI is 0.21. So, the structure shows high FOM and the FOM is obtained about 10,660.

7 Conclusion

In this paper, we have developed a novel structure for the optical absorber with a wide bandwidth and high FOM value for optical spectrum. We have demonstrated how the capacitance can be considered for controlling the bandwidth of the absorber. The parametric studies are helpful to optimize the absorber by controlling the capacitance. Our proposed structure has a bandwidth of 28% and a reflection value of around -47 dB which makes it superior over other models. The symmetrical formation of the absorber provides the polarization independence. Moreover, the shift of the frequency and reflection value is used for calculating the FOM which is obtained around 10,660.

References

- Adato, R., Yanik, A.A., Altug, H.: On chip plasmonic monopole nano-antennas and circuits. *Nano Lett.* **11**(12), 5219–5226 (2011)
- Adato, R., Aksu, S., Altug, H.: Engineering mid-infrared nanoantennas for surface enhanced infrared absorption spectroscopy. *Mater. Today* **18**(8), 436–446 (2015)
- Barzegar-Parizi, S.: Realization of wide-angle and wideband absorber using metallic and graphene-based metasurface for mid-infrared and low THz frequency. *Opt. Quant. Electron.* **50**(10), 378 (2018)
- Bazgir, M., Novin, S.N., Zarrabi, F.B., Heydari, S., Arezoomand, A.S.: A novel plasmonic elliptical nano-cluster and investigating Fano response in π - and T-shaped arrays. *Electromagnetics* **38**(4), 207–216 (2018)
- Cen, C., Chen, J., Liang, C., Huang, J., Chen, X., Tang, Y., Yi, Z., Xu, X., Yi, Y., Xiao, S.: Plasmonic absorption characteristics based on dumbbell-shaped graphene metamaterial arrays. *Phys. E* **103**, 93–98 (2018)
- Cetin, A.E., Turkmen, M., Aksu, S., Etezadi, D., Altug, H.: Multi-resonant compact nanoaperture with accessible large nearfields. *Appl. Phys. B* **118**(1), 29–38 (2015)

- Chen, J., Yi, Z., Xiao, S., Xu, X.: Absorption enhancement in double-layer cross-shaped graphene arrays. *Mater. Res. Express* **5**(1), 015605 (2018)
- Chiadini, F., Fiumara, V., Scaglione, A., Lakhtakia, A.: Compound surface-plasmon-polariton waves guided by a thin metal layer sandwiched between a homogeneous isotropic dielectric material and a structurally chiral material. *Opt. Commun.* **363**, 201–206 (2016)
- Durmaz, H., Li, Y., Cetin, A.E.: A multiple-band perfect absorber for SEIRA applications. *Sens Actuators B Chem.* **275**, 174–179 (2018)
- Etchegoin, P.G., Le Ru, E.C., Meyer, M.: An analytic model for the optical properties of gold. *J. Chem. Phys.* **125**(16), 164705 (2006)
- Falcone, F., Lopetegi, T., Laso, M.A.G., Baena, J.D., Bonache, J., Beruete, M., Marqués, R., Martín, F., Sorolla, M.: Babinet principle applied to the design of metasurfaces and metamaterials. *Phys. Rev. Lett.* **93**(19), 197401 (2004)
- Farmani, A., Mir, A., Bazgir, M., Zarrabi, F.B.: Highly sensitive nano-scale plasmonic biosensor utilizing Fano resonance metasurface in THz range: numerical study. *Phys. E* **104**, 233–240 (2018)
- Ghasemi, M., Choudhury, P.K.: Nanostructured concentric gold ring resonator-based metasurface filter device. *Opt. Int. J. Light Electron Opt.* **127**(20), 9932–9936 (2016)
- Giannini, V., Fernández-Domínguez, A.I., Heck, S.C., Maier, S.A.: Plasmonic nanoantennas: fundamentals and their use in controlling the radiative properties of nanoemitters. *Chem. Rev.* **111**(6), 3888–3912 (2011)
- Gomez-Diaz, J.S., Tymchenko, M., Lee, J., Belkin, M.A., Alù, A.: Nonlinear processes in multi-quantum-well plasmonic metasurfaces: electromagnetic response, saturation effects, limits, and potentials. *Phys. Rev. B* **92**(12), 125429 (2015)
- Hedayati, M.K., Faupel, F., Elbahri, M.: Review of plasmonic nanocomposite metamaterial absorber. *Materials* **7**(2), 1221–1248 (2014)
- Heydari, S., Bazgir, M., Zarrabi, F.B., Gandji, N.P., Rastan, I.: Novel optical polarizer design based on metasurface nano aperture for biological sensing in mid-infrared regime. *Opt. Quant. Electron.* **49**(2), 83 (2017a)
- Heydari, S., Rastan, I., Parvin, A., Pirooj, A., Zarrabi, F.B.: Investigation of novel fractal shape of the nano-aperture as a metasurface for bio sensing application. *Phys. Lett. A* **381**(3), 140–144 (2017b)
- Hu, X., Dauler, E.A., Molnar, R.J., Berggren, K.K.: Superconducting nanowire single-photon detectors integrated with optical nano-antennae. *Opt. Express* **19**(1), 17–31 (2011)
- Jafari, F.S., Ahmadi-Shokouh, J.: Frequency-selective surface to determine permittivity of industrial oil and effect of nanoparticle addition in x-band. *J. Electron. Mater.* **47**(2), 1397–1404 (2018)
- Jahangiri, P., Zarrabi, F.B., Naser-Moghadasi, M., Arezoomand, A.S., Heydari, S.: Hollow plasmonic high Q-factor absorber for bio-sensing in mid-infrared application. *Opt. Commun.* **394**, 80–85 (2017)
- Kang, M., Liu, F., Li, T.-F., Guo, Q.-H., Li, J., Chen, J.: Polarization-independent coherent perfect absorption by a dipole-like metasurface. *Opt. Lett.* **38**(16), 3086–3088 (2013)
- Liu, N., Mesch, M., Weiss, T., Hentschel, M., Giessen, H.: Infrared perfect absorber and its application as plasmonic sensor. *Nano Lett.* **10**(7), 2342–2348 (2010)
- Lu, C., Hu, X., Yue, S., Fu, Y., Yang, H., Gong, Q.: Ferroelectric hybrid plasmonic waveguide for all-optical logic gate applications. *Plasmonics* **8**(2), 749–754 (2013)
- Mayer, K.M., Hafner, J.H.: Localized surface plasmon resonance sensors. *Chem. Rev.* **111**(6), 3828–3857 (2011)
- Meinzer, N., Barnes, W.L., Hooper, I.R.: Plasmonic meta-atoms and metasurfaces. *Nat. Photonics* **8**(12), 889–898 (2014)
- Mirzabeygi, M., Naser-Moghadasi, M.: Investigation the hexagonal cylindrical absorber for bio-sensing in optical regime. *Opt. Quant. Electron.* **50**(2), 63 (2018)
- Muhammad, M.H., Hameed, M.F.O., Obayya, S.S.A.: Broadband absorption enhancement in periodic structure plasmonic solar cell. *Opt. Quant. Electron.* **47**(6), 1487–1494 (2015)
- Nouri-Novin, S., Zarrabi, F.B., Eskandari, A.-R., Naser-Moghadasi, M.: Design of a plasmonic absorber based on the nonlinear arrangement of nanodisk for surface cloak. *Opt. Commun.* **420**, 194–199 (2018)
- Nozhat, N., Granpayeh, N.: Switching power reduction in the ultra-compact Kerr nonlinear plasmonic directional coupler. *Opt. Commun.* **285**(6), 1555–1559 (2012)
- Rufangura, P., Sabah, C.: Wide-band polarization independent perfect metamaterial absorber based on concentric rings topology for solar cells application. *J. Alloys Compd.* **680**, 473–479 (2016)
- Simovski, C., Morits, D., Voroshilov, P., Guzhva, M., Belov, P., Kivshar, Y.: Enhanced efficiency of light-trapping nanoantenna arrays for thin-film solar cells. *Opt. Express* **21**(104), A714–A725 (2013)
- Tittel, A., Kremers, C., Dorfmueller, J., Chigrin, D.N., Giessen, H.: Spectral shifts in optical nanoantenna-enhanced hydrogen sensors. *Opt. Mater. Express* **2**(2), 111–118 (2012)

- Watanabe, T., Tombet, S.B., Tanimoto, Y., Wang, Y., Minamide, H., Ito, H., Fateev, D., et al.: Ultrahigh sensitive plasmonic terahertz detector based on an asymmetric dual-grating gate HEMT structure. *Solid State Electron.* **78**, 109–114 (2012)
- Withayachumnankul, W., Shah, C.M., Fumeaux, C., Ung, B.S.-Y., Padilla, W.J., Bhaskaran, M., Abbott, D., Sriram, S.: Plasmonic resonance toward terahertz perfect absorbers. *ACS Photonics* **1**(7), 625–630 (2014)
- Xu, H., Li, H., Xiao, G.: Plasmonic resonance in planer split ring trimer. *Opt. Commun.* **332**, 144–148 (2014)
- Yang, D., Tian, H., Ji, Y.: The study of electro-optical sensor based on slotted photonic crystal waveguide. *Opt. Commun.* **284**(20), 4986–4990 (2011)
- Zare, M.S., Nozhat, N., Rashiditabar, R.: Tunable graphene based plasmonic absorber with grooved metal film in near infrared region. *Opt. Commun.* **398**, 56–61 (2017)
- Zarrabi, F.B., Bazgir, M., Ebrahimi, S., Arezoomand, A.S.: Fano resonance for UI nano-array independent to the polarization providing bio-sensing applications. *J. Electromagn. Waves Appl.* **31**(14), 1444–1452 (2017)
- Zhao, Y., Alù, A.: Manipulating light polarization with ultrathin plasmonic metasurfaces. *Phys. Rev. B* **84**(20), 205428 (2011)
- Zheng, G., Zou, X., Chen, Y., Xu, L., Rao, W.: Fano resonance in graphene-MoS₂ heterostructure-based surface plasmon resonance biosensor and its potential applications. *Opt. Mater.* **66**, 171–178 (2017)